Published in final edited form as:
*J Biomed Mater Res A*. 2010 May ; 93(2): 807–816. doi:10.1002/jbm.a.32769.

# Identification of Osteoconductive and Biodegradable Polymers from a Combinatorial Polymer Library

**Darren M. Brey**[1], **Cindy Chung**[1], **Kurt D. Hankenson**[2], **Jonathon P. Garino**[3], and **Jason A. Burdick**[1]

[1]University of Pennsylvania, School of Engineering and Applied Science, Department of Bioengineering, Philadelphia, PA 19104

[2]Department of Animal Biology, School of Veterinary Medicine, University of Pennsylvania, Philadelphia, PA 19103

[3]University of Pennsylvania Medical Center, Department of Orthopaedics, Philadelphia, PA 19104

## Abstract

Combinatorial polymer syntheses are now being utilized to create libraries of materials with potential utility for a wide variety of biomedical applications. We recently developed a library of photopolymerizable and biodegradable poly(β-amino ester)s (PBAEs) that possessed a range of tunable properties. In this work, the PBAE library was assessed for candidate materials that met design criteria (e.g., physical properties such as degradation and mechanical strength and *in vitro* cell viability and osteoconductive behavior) for scaffolding in mineralized tissue repair. The most promising candidate, A6, was then processed into 3-dimensional porous scaffolds and implanted subcutaneously and only presented a mild inflammatory response. The scaffolds were then implanted intramuscularly and into a critically-sized cranial defect either alone or loaded with bone morphogenetic protein-2 (BMP-2). The samples in both locations displayed mineralized tissue formation in the presence of BMP-2, as evident through radiographs, micro-computed tomography, and histology, while samples without BMP-2 showed minimal or no mineralized tissue. These results illustrate a process to identify a candidate scaffolding material from a combinatorial polymer library, and specifically for the identification of an osteoconductive scaffold with osteoinductive properties via the inclusion of a growth factor.

### Keywords

combinatorial library; polymers; osteoconductivity; photopolymerization; Biodegradable

## 1. Introduction

Traditional polymer development for tissue engineering applications has been a time consuming and tedious process, as polymer synthesis often requires multiple reactions and purification steps. Fortunately, technology is continuously being developed to accelerate various steps in the tissue engineering process, including the high-throughput screening of materials and small molecule mediators of cellular behavior, the use of microdevices to screen cellular microenvironments, technology to rapidly assess material properties, and the use of combinatorial polymer syntheses.[1] In general, combinatorial synthesis is a method to produce large libraries of compounds and materials through simplified single-step

Corresponding Author: Jason A. Burdick, Ph.D., Department of Bioengineering, University of Pennsylvania, 240 Skirkanich Hall, 210 South 33rd Street, Philadelphia, PA 19104 USA, burdick2@seas.upenn.edu.

reactions.[2] This approach has been used widely in the pharmaceutical industry to greatly expand the pool of drugs for investigation, and to help identify structure-property relationships of bioactive molecules.[3]

More recently, combinatorial libraries are being utilized to develop materials for biomedical applications; including gene delivery vehicles,[4,5] substrates for the culture of stem cells,[6,7] and potential biodegradable materials for tissue engineered scaffolds.[8–12] For scaffold development, combinatorial syntheses are able to produce libraries of materials that can be screened and developed for a specific application based on desired properties. For example, Brocchini *et al.* developed a library of 112 polyarylates that exhibited a range of physical and cellular characteristics.[9] This library has been used to develop predictive computational models of chemical structures and physical properties,[13] cell growth,[14] and protein adsorption.[15] These models were then utilized to virtually design a polymethacrylate combinatorial library that predicted cell attachment, cell growth, and fibrinogen adsorption.[13] Experimentally measured values showed agreement in many of the predicted properties, which opens the door for future, faster and cheaper biomaterial development procedures.

Beyond distinct chemical libraries, gradients of materials may also be used to identify optimal formulations to meet a given set of criteria. Using these approaches, both Meredith *et al.* and and Yang *et al.* were able to optimize the combination of poly(D,L-lactide) and poly(ε-caprolactone)[10] and tyrosine-derived polycarbonates,[11] respectively, for desirable osteoblast interactions. Additionally, combinatorial synthesis on the nanoliter scale can greatly accelerate material discovery. For example, 3456 different individual combinations and ratios of 24 polymers were mixed in nanoliter spots on an array in order to determine cell-material interactions.[7]

An important step in this approach is the identification of effective criteria that permit material selection for specific applications. For tissue engineering, these criteria may include properties such as: degradation rate, mechanics, cell attachment, cytotoxicity, and biocompatibility.[16] Degradation allows a material to be replaced with cells and tissue over time, but is also important for the temporal mechanical properties and the release of degradation products. Mechanical properties are important for the stability of a scaffold, but have also been implicated in the differentiation of cells (e.g., mesenchymal stem cells, MSCs).[17] Additionally, mechanical mismatching can lead to issues such as stress shielding, which weakens the surrounding bone in orthopaedic applications.[18] Cell attachment is needed for matrix deposition by anchorage dependent cells and can be facilitated through protein adsorption, such as fibronectin, or through the incorporation of known cell binding peptides (i.e., RGD).[19] Biocompatibility can indicate that a material does not incur any significant inflammatory or immune response when implanted into the body.[20] Also, it is desirable for a material to not just be isolated from the body through a foreign body response, but to also integrate with tissues.[20] ‘Bioactive’ materials can be designed to support certain tissues or even be used to help drive differentiation with the addition of functional groups.[21]

With these issues in mind, we recently developed a combinatorial library of acrylate-terminated poly(β-amino ester)s (PBAEs) that form networks with a wide range of mechanical properties (3–300 MPa) and degradation rates (<24 hours to >100 days) based on chemical variations.[8] The macromers were formed through simple addition reactions without the need for purification, and thus meet the criteria for combinatorial synthesis. Additionally, the size and branching of the macromers was modified to introduce further material control for a desired application.[22,23] These macromers can be crosslinked into networks using a radical polymerization (e.g., photopolymerization)[24] and can be processed

into 3-dimensional scaffolds using basic templating/poragen techniques[23] or through electrospinning into fibrous structures.[25]

The diversity of this PBAE library allows for exploration for a range of tissue engineering applications, and in this work, the library was screened to identify an osteoconductive material for use in mineralized tissue regeneration. The candidates were first assessed for material properties and *in vitro* cellular interactions and an optimal candidate was processed into 3-dimensional scaffolds and implanted into rat cranial defects to assess the bone regeneration potential. An osteoinductive factor was also introduced to further illustrate the potential of the scaffold for mineralized tissue growth. This work has identified a novel biomaterial with beneficial characteristics for promoting bone regeneration; but perhaps more importantly, it illustrates a process that can be used for developing tissue engineering scaffolds from combinatorial libraries of biodegradable polymers.

## 2. Materials and methods

### 2.1. Macromer synthesis

PBAEs were synthesized as described previously.[8] Briefly, 10 combinations of diacrylates and primary amines (all reagents were purchased from Sigma, Scientific Polymer Products, or TCI America) were chosen from previous data[8] according to their degradation rate to meet design criteria and mixed together in a molar ratio of 1.2:1, respectively, overnight at 90°C. The reaction scheme and reagents used are shown in Figure 1 and the sample notation is from the original study on the library development.[8] The macromers were characterized with proton nuclear magnetic resonance ($^1$H NMR, Bruker DMX360, 360 MHz) and were determined to be ~2 kDa. The photoinitiator 2,2-dimethoxy-2-phenyl acetophenone (DMPA, Sigma) was added to the liquid macromers at a final concentration of 0.5% (w/w). The viscous macromer solutions were then polymerized with exposure to ultraviolet light (~10 mW/cm$^2$, 365 nm, 10 min, Blak-Ray B-100 AP).

### 2.2. In vitro characterization

Bulk slabs were obtained by polymerizing the macromers between two glass slides with a 1 mm thick spacer and cutting samples to a desired size. Mass loss was monitored by placing 8 × 12 mm samples into phosphate buffered saline (PBS) at a pH of 7.4 on an orbital shaker at 37°C. At desired time points, the samples were removed, lyophilized, and the final mass compared to the initial mass. The mechanical properties of the materials were assessed by compression of 5 mm diameter disks with a dynamic mechanical analyzer (Q800 TA Instruments) at a strain rate of 10%/min with the modulus determined as the slope of the stress/strain curve at low strains (<20%).

To form thin films, macromers were dissolved in ethanol at 1:2 (wt/vol macromer:EtOH), added to 24-well plates (30 μl), the ethanol was allowed to evaporate overnight, and the macromer was crosslinked with UV exposure in a nitrogen environment. Human MSCs (Lonza) were seeded on the films at a density of 5000 cells/cm$^2$ and cultured for up to 7 days. MSCs were cultured in growth media (αMEM, 17% fetal bovine serum, 1% penicillin/streptomycin, 1% l-glutamine) or osteogenic media (growth media, 10 mM β-glycerol phosphate, 25 μg/mL ascorbic acid-2-phosphate, 10 nM dexamethasone). Viability was measured using a metabolic activity assay (Alamar Blue, Invitrogen), by adding 50 μl of the reagent to each well, incubating for 4 hours, and reading the fluorescence in a plate reader (Bio-Tek Synergy HT, excitation-545 nm, emission-590 nm). Osteogenic differentiation and activity of the MSCs in osteogenic media was measured with an alkaline phosphatase fluorescent assay (APF, Sigma), following manufacturer's protocols, as alkaline phosphatase is an early indicator of bone formation.

Cells were then cultured on the best candidate material over 3 weeks to further characterize the osteoconductivity of the materials. RNA was extracted at 7, 14, and 19 days using TRIzol® (Invitrogen) and isolated according to manufacturer's instructions. RNA concentration and quality were determined using an ND-1000 spectrometer (Nanodrop Technologies) and 1 ug of RNA was reverse transcribed into cDNA using reverse transcriptase (Superscript II, Invitrogen) and OligoDT (Invitrogen). The relative gene expression was determined using an Applied Biosystems 7300 Real-Time Polymerase Chain Reaction system for osteocalcin and normalized to the housekeeping gene glyceraldehyde 3-phosphate dehydrogenase (GAPDH, Table 1) followed by normalization to the cell pellet gene expression levels at day 0 using the $\Delta\Delta C_T$ method.

### 2.3. In vivo characterization

Sprague Dawley (250–275 g, Charles River) rats were used and NIH guidelines for the care and use of laboratory animals (NIH Publication #85-23 Rev. 1985) were observed. Polymer disks (n = 3, 8 mm diameter, 1 mm thick) were implanted subcutaneously into dorsal pockets in rats for 2, 4, and 8 weeks to monitor *in vivo* degradation and investigate the inflammatory response of the local tissue as performed previously.[26] Scaffolds were prepared using a bead sintering and extraction procedure as described previously.[23] Briefly, ~200 μm diameter PMMA beads (Polysciences) were sintered overnight in an 8 mm × 1.5 mm teflon mold, the macromer/initiator was added to fill the void spaces, and the sample was photopolymerized with UV exposure between two glass slides. The PMMA beads were removed with serial washes in methylene chloride and then the methylene chloride was evaporated from scaffolds in a fume hood. Scaffolds (n = 3) were characterized with scanning electron microscopy (SEM, JEOL 7500 HR-SEM) and were implanted subcutaneously to confirm tissue infiltration and to investigate the tissue response.

These scaffolds (1.5 mm thick) were then used as composites by adding a small amount (61 μl) of collagen (Inamed Biomaterials) into the pores either alone or loaded with 2 μg of rhBMP-2 (R&D systems). The collagen solution was allowed to gel at 37°C for 1.5 hours and the scaffolds were frozen and lyophilized. Scaffolds were then implanted either intramuscularly (6 mm diameter) or into a critical-sized cranial defect (8 mm diameter) in rats. For the intramuscular implants, scaffolds (A6 porous scaffolds with and without BMP-2) were implanted bilaterally into the adductor thigh muscle for 4 weeks.[27] For cranial implants, an 8 mm defect was made using a hand trephine across the sagittal suture, and A6 scaffolds were placed into the defects. Four groups were investigated (n = 5/group) including empty defects, defects filled with porous scaffold alone, defects filled with porous scaffold containing a small amount of collagen gel, and defects filled with polymer scaffold containing a small amount of collagen gel loaded with BMP-2. Calvaria were removed at 6 weeks and fixed in 4% formalin.

High-resolution x-ray images were obtained using an MX-20 Faxitron (15 s and 25 kV). The radiopacity was measured as the percent intensity of the defect area over the intensity of intact bone and analyzed with ImageJ software. Calvaria were then scanned using a VivaCT40 uCT scanner (Scanco) with X-ray acquisition settings set at 55 kVp and 145 mA and an integration time of 200 ms. Scans were performed with an isotropic voxel size of 10.5 μm and images were reconstructed in 1024 × 1024 pixel matrices. A lower threshold of 743.4 mg/cm$^3$ and an upper threshold of 2000 mg/cm$^3$ were determined by visual inspection to best distinguish between bone and non-bone material. Scanco computer software was used to calculate the bone volume and the connectivity index. Samples were then decalcified in 10% EDTA for 3 weeks, dehydrated, and then mounted in paraffin wax for histology. Samples were processed using standard techniques for hematoxylin and eosin staining.

### 2.4. Statistics

Statistical analysis was performed using ANOVA with Tukey's post-hoc among the groups with significance defined as a p-value less than 0.05. All values are reported as the mean and the standard deviation of the mean.

## 3. Results and discussion

### 3.1. Polymer development

As technology to rapidly produce large numbers of materials (e.g., combinatorial libraries) is developed, it is important to understand the process to identify optimal materials for desired applications. For this work, a previously developed library of PBAEs was assessed to identify osteoconductive materials for use as scaffolding in mineralized tissue regeneration. The PBAE macromers are synthesized by the conjugate addition of commercially available amines and diacrylates (Figure 1), without the production of byproducts that would need purification; thus, large numbers of molecules are rapidly produced. Due to the availability of vasculature and progenitor cells in bone[16], there is the potential for acellular approaches that rely on the recruitment of these localized resources to scaffolding that is conducive to cellular interactions and may also include inductive cues to stimulate osteogenesis. This may be advantageous for many instances over cellular approaches that would be patient specific and require additional steps prior to implantation. Thus, our approach is to identify an osteoconductive material from the library with the appropriate physical properties and cellular interactions and then to include osteoinductive molecules to further improve tissue regeneration.

For tissue engineering, the scaffold supports cell adhesion and acts as a template to control the geometry and extent of produced tissue. Ideally, this material would degrade with time and be replaced with new tissue. This can be a delicate balance as losing mass too quickly could prevent adequate cell adhesion and support, whereas too slowly could inhibit the normal growth and replacement of natural tissue[28]. With this in mind, the desired degradation behavior for this application was determined to be gradual mass loss and complete degradation within approximately 3–5 months. This will hopefully allow for minimal toxicity from the degradation products, yet provide support during the approximate time for a fracture to heal and the bony callus to resorb.[29,30]

From the original PBAE library of 120 polymers, 10 macromers (Figure 1: A6, A7, B1, B2, C11, C12, E1, E2, E9, and J6) were identified as forming polymer networks that meet this mass loss criteria. The shapes of the degradation profiles (Figure 2A) ranged from fairly linear to a more rapid initial release followed by a slower plateau region. Differences may be attributed to variability in the hydrophobicity of the polymers, which could affect the rate of water uptake and hydrolysis, or the presence of a soluble fraction that may be released rapidly. A slower initial degradation may also be preferable as it allows cells to populate scaffolds before the substrate begins to degrade and the network properties change.

The compressive moduli for slabs of these 10 polymer networks are shown in Figure 2B. The variation of this subset of materials was all in the same order of magnitude (~0.5 to 4.0 MPa), in contrast to the entire library which ranged over two orders of magnitude.[8] The mechanical properties are important to the cellular microenvironment, as previous studies have shown that stem cells grown on stiffer substrates differentiate towards an osteogenic pathway, while cells that are grown on very soft surfaces differentiate towards other lineages.[17] The low modulus of these materials with respect to bone, as with all synthetic polymer systems, will restrict utility to non-load bearing defects or use in conjunction with other fixation techniques. The A6 network had the highest moduli of the 10 polymers, at 3.8

± 0.3 MPa; however, since all of these samples possessed moduli in the same magnitude, mechanics were not used to exclude any candidates from the group.

### 3.2. Cellular interactions in vitro

Next, the ability of cells to adhere and remain viable on the surfaces of these materials was investigated by growing MSCs on thin films of polymers and measuring the cellular metabolic activity (with the Alamar Blue assay), as reported in Figure 3A. The media in the wells with C11 and C12 quickly changed to yellow, indicating an acidic environment in which the cells did not survive. Similarly, cells grown on A7 did not remain viable and the polymer E9 prematurely crosslinked and could not be further assessed. Therefore, these four materials were removed from further testing. Cellular mitochondrial activity increased for other groups (B1, B2, E2, J6), but decreased between the 4 and 7 day time points. However, the mitochondrial activity steadily increased for polymers E1 and A6 over the entire week of culture. Variations in the mitochondrial activity between polymers may be attributed to a number of factors including changes in protein adsorption, which can affect initial adhesion events, or the toxicity of degradation products that are eluted at different times in culture. However, the presence of cells at the 7 day time point and proliferation with culture has generally been a good indicator of non-toxicity in these environments.

Alkaline phosphatase (ALP) activity of MSCs grown on polymer thin films after 3 days in osteogenic media (Figure 3B) was used as one measure of the osteoconductivity of these polymers. Although ALP activity was observed by cells on all of these polymers, the ALP activity of the cells grown on A6 was significantly greater than the activity of the cells on all other polymers except B2. Comparing the A6 and B2 polymers, the A6 supported a steady increase in cell viability throughout the 1 week period and was higher after 7 days. B2 and A6 had relatively similar linear degradation profiles, but A6 had a modulus that was roughly double that of polymer B2. With these factors in mind, A6 was selected for further analysis as an osteoconductive polymer from the library.

Osteoconductivity was also assessed by measuring osteocalcin gene expression of MSCs cultured on films of A6. The osteocalcin expression (Figure 4) greatly increased from the initial level throughout the duration of the experiment, and was significantly greater for MSCs on A6 than MSCs grown on control tissue culture polystyrene (TCPS) at 2 and 3 weeks. Osteocalcin is an important non-collagenous matrix protein specific to bone, and an increased expression of 17.4 ± 11.0 and 3.95 ± 1.17 fold at 2 and 3 weeks, respectively, should indicate increased mineralized tissue production. The up-regulation in osteocalcin is supported by the increase in ALP expression found in the shorter term studies.

### 3.3. Scaffold formation and assessment subcutaneously

A longer term degradation study showed that the A6 polymer was completely degraded after 17 weeks in PBS (Figure 5A), which fits our 3–5 month degradation criteria. For comparison, bulk slabs of A6 were implanted subcutaneously in rats to measure their inflammatory response, as well as the *in vivo* degradation profile. The mass loss behavior of these samples *in vivo* was similar to what was observed *in vitro*, especially at 2 and 8 weeks (Figure 5A), with ~50% mass lost after 8 weeks. Histological images of the A6 implants after 4 and 8 weeks are shown in Figure 5B and C, respectively. The polymer elicited a mild inflammatory response in the first 2 weeks with some new blood vessel formation and macrophage recruitment to the polymer-tissue interface. With time, the polymer was encapsulated with thin fibrous tissue, and there is no evidence of inflammation or necrosis within the adjacent subcutaneous fibroadipose tissue, skin adnexal structures or deep skeletal muscle. In general, these results indicate a mild inflammatory response, typical of commonly used biodegradable and biocompatible polymers.

Towards utility in 3-dimensional tissue engineering, porous A6 scaffolds (Figure 5D) were fabricated using a previously described poragen leaching technique.[23] Scaffolds exhibited large pores (~200 μm) and pore interconnectivity, both of which are important design parameters for musculoskeletal tissue scaffolds.[16,31] When implanted subcutaneously, minimal inflammation was observed and tissue fully infiltrated the acellular scaffolds (Figure 5E). Histological assessment revealed that this tissue was fibrous and vascularized and there was no indication of mineralized tissue production within the scaffold, which is not expected without incorporation of inductive cues.

### 3.4. Bone formation in vivo

An important component for many tissue engineering approaches is the incorporation of inductive factors, such as direct recombinant growth factor delivery or through gene therapy.[32] In many cases, scaffolds incorporating these inductive factors improve their ability to produce functional tissue. In this work, we introduced a known, FDA-approved osteoinductive factor (BMP-2)[33,34] into the porous scaffolds by loading the molecule within a very small amount of collagen. The collagen solution is simply pipetted into the porous scaffold and gelled with elevated temperature. The collagen is easily remodeled by cells and the BMP-2 is released through both diffusion and cell-mediated degradation. This made it difficult to quantify the specific release profiles obtained with this technique.

Two models were used for the evaluation of these BMP-2 loaded osteoconductive scaffolds. First, the scaffolds were implanted into an intramuscular implant site, as described by Hartman *et al*,[27] to assess their ability to form ectopic mineralized tissue. For this experiment, only two groups were tested, A6 scaffold with BMP-2 loaded collagen and the A6 scaffold with collagen alone, implanted for 4 weeks. The radiographs in Figure 6A (no BMP-2) and Figure 6B (with BMP-2, looking from a side view) indicate that ectopic mineralized tissue is formed, but only in the scaffolds incorporating the osteoinductive factor. Likewise, histology of implants without BMP-2 show no evidence of bone formation (Figure 6C), yet mineralized tissue is observed in the BMP-2 loaded scaffolds (Figure 6D). 3D reconstruction of the newly produced bone using μCT demonstrates extensive mineralization with a pattern that resembles the interconnected pores of the scaffold.

The scaffolds were further assessed in a critical-sized cranial defect (8 mm) model in rats that does not support extensive healing without intervention.[35] The defect is not load bearing, and is common to the intramembranous bone healing of fractures that are rigidly fixed.[36,37] Four groups were assessed; the negative control of an empty defect, the A6 scaffold alone, the A6 scaffold plus collagen gel, and the A6 scaffold plus collagen gel loaded with 2 μg of BMP-2. Treatments of collagen gel alone were not assessed since it would involve significantly more collagen to fill the defect site than what is used as a BMP-2 carrier in the pores and would not be a relevant comparison. After 6 weeks, radiographs (Figure 7A) indicate that only the samples loaded with BMP-2 had consistent bone growth throughout the scaffold, while the other groups showed minimal growth, mostly at the outer edges. The radiopacity (Figure 7B) of samples with BMP-2 was significantly greater than the other 3 groups, and there were no significant differences between these other groups.

Similarly, μCT images (Figure 8A) show consistent bone growth in the samples with BMP-2. Again, while there is some growth in the empty defects, the cross sections show that this is very thin and only at the edges. The bone volume (Figure 8B) showed similar results to the radiographic data, with significantly greater bone volume in the BMP-2 containing samples at $16.4 \pm 4.1\ mm^3$ compared to other groups. The connectivity index (Figure 8C), a measure of the interconnectivity of the bone, is significantly higher in the BMP-2 samples as well. Finally, histological samples of A6 scaffolds (Figure 9) reinforced the μCT data. In the

untreated defects, there is some growth of bone, but the majority of the defect is filled with thin fibrous tissue. In the scaffolds without growth factor (regardless of the presence of collagen), there is tissue infiltration throughout the scaffolds, but the only bone growth is observed at the edges of the scaffold. In the BMP-2 scaffolds, there is bone formation within the scaffold consistently from the outer edge all the way through to the middle.

The samples with BMP-2 showed bone formation throughout the scaffold and the bone was connected throughout due to the interconnectivity of the pores created by the sintered microbeads. At 6 weeks, the new bone is still interdispersed within the remaining A6 scaffold. There is no evidence of cartilage, potentially since the bone is forming through intramembranous ossification or perhaps because of the later time points of harvest. BMP-2 greatly enhanced new bone formation within the scaffold, and could have recruited progenitor cells in the area to differentiate along an osteogenic lineage to produce mineralized tissues. There was no significant difference in the amount of bone formed in any of the other groups, and the bone that was formed was largely restricted to the perimeter of the defect. Thus, it is believed that while the porous scaffolds identified as being conductive supported tissue growth and did not possess a highly inflammatory response, they do not have any inherent inductive capabilities.

The use of combinatorial libraries can greatly increase the pool of materials for use in biomedical applications. In this case, a relatively small but diverse set of PBAEs was screened for use in mineralized tissue engineering, but this library could also be used in the development of materials for drug delivery, gene delivery,[4] or other tissue engineering applications.[25] The tunability of properties through control of macromer synthesis[22,23] and the flexibility afforded to the processing of photopolymerizable materials reflect the advantages of this particular library. This screen was accomplished with a relatively straight-forward approach using traditional bulk measurements of degradation, mechanics, and cell viability. The complexity of this system can be quickly increased by investigating copolymers of the library constituents or investigating gradients of monomers. The use of techniques that more rapidly screen these parameters, including with microdevices, will be important in identifying materials for given applications in the future.

## 4. Conclusions

By screening a library of 120 photocrosslinked PBAEs against design parameters (bulk properties, cellular adhesion and toxicity) for an application of mineralized tissue engineering, an osteoconductive material was identified. Cells cultured on this optimal material exhibited enhanced viability profiles and alkaline phosphatase activity compared to other polymers. When implanted subcutaneously, the material elicited minimal inflammation, and porous scaffolds were fully infiltrated with tissue. While this material has no inherent osteoinductive properties, it was loaded with a known osteoinductive factor, BMP-2, which led to bone formation ectopically in an intramuscular location and within a critical-sized bone defect. This work presents a process for identifying potential scaffolding material for tissue engineering applications using a combinatorial library of biodegradable macromers that can be crosslinked into networks.

## Acknowledgments

Support for this research was provided through a Department of Veterans Affairs Research Grant, a Development Grant Award from the Center for Research in FOP and Related Disorders at the University of Pennsylvania, and a grant from the National Institutes of Health (R01 DE017471 to KDH). The authors would like to acknowledge Jamie Ifkovits for assistance in running SEM, Bryan Marguiles for assistance in running μCT, and Dr. Robert Padera for assistance with analyzing histology.

## References


1. Peters A, Brey DM, Burdick JA. High-throughput and Combinatorial Technologies for Tissue Engineering Applications. Tissue Engineering, Part B. 2009; 15:225–239.
2. Hoogenboom R, Meier MAR, Schubert US. Combinatorial methods, automated synthesis and high-throughput screening in polymer research: Past and present. Macromolecular Rapid Communications. 2003; 24(1):16–32.
3. Goldberg M, Mahon K, Anderson D. Combinatorial and rational approaches to polymer synthesis for medicine. Advanced Drug Delivery Reviews. 2008; 60(9):971–978. [PubMed: 18423930]
4. Lynn DM, Anderson DG, Putnam D, Langer R. Accelerated discovery of synthetic transfection vectors: Parallel synthesis and screening of degradable polymer library. Journal of the American Chemical Society. 2001; 123(33):8155–8156. [PubMed: 11506588]
5. Putnam D. Polymers for gene delivery across length scales. Nature Materials. 2006; 5(6):439–451.
6. Anderson DG, Levenberg S, Langer R. Nanoliter-scale synthesis of arrayed biomaterials and application to human embryonic stem cells. Nature Biotechnology. 2004; 22(7):863–866.
7. Anderson DG, Putnam D, Lavik EB, Mahmood TA, Langer R. Biomaterial microarrays: rapid, microscale screening of polymer-cell interaction. Biomaterials. 2005; 26(23):4892–4897. [PubMed: 15763269]
8. Anderson DG, Tweedie CA, Hossain N, Navarro SM, Brey DM, Van Vliet KJ, Langer R, Burdick JA. A combinatorial library of photocrosslinkable and degradable materials. Advanced Materials. 2006; 18(19):2614–2618.
9. Brocchini S, James K, Tangpasuthadol V, Kohn J. A combinatorial approach for polymer design. Journal of the American Chemical Society. 1997; 119(19):4553–4554.
10. Meredith JC, Sormana JL, Keselowsky BG, Garcia AJ, Tona A, Karim A, Amis EJ. Combinatorial characterization of cell interactions with polymer surfaces. Journal of Biomedical Materials Research Part A. 2003; 66A(3):483–490. [PubMed: 12918030]
11. Yang Y, Bolikal D, Becker ML, Kohn J, Zeiger DN, Simon CG. Combinatorial polymer scaffold libraries for screening cell-biomaterial interactions in 3D. Advanced Materials. 2008; 20(11):2037. +
12. Khademhosseini A, Langer R, Borenstein J, Vacanti JP. Microscale technologies for tissue engineering and biology. Proceedings of the National Academy of Sciences of the United States of America. 2006; 103(8):2480–2487. [PubMed: 16477028]
13. Brocchini S, James K, Tangpasuthadol V, Kohn J. Structure-property correlations in a combinatorial library of degradable biomaterials. Journal of Biomedical Materials Research. 1998; 42(1):66–75. [PubMed: 9740008]
14. Abramson SD, Alexe G, Hammer PL, Kohn J. A computational approach to predicting cell growth on polymeric biomaterials. Journal of Biomedical Materials Research Part A. 2005; 73A(1):116–124. [PubMed: 15714501]
15. Gubskaya AV, Kholodovych V, Knight D, Kohn J, Welsh WJ. Prediction of fibrinogen adsorption for biodegradable polymers: Integration of molecular dynamics and surrogate modeling. Polymer. 2007; 48(19):5788–5801. [PubMed: 19568328]
16. Agrawal CM, Ray RB. Biodegradable polymeric scaffolds for musculoskeletal tissue engineering. Journal of Biomedical Materials Research. 2001; 55(2):141–150. [PubMed: 11255165]
17. Engler AJ, Sen S, Sweeney HL, Discher DE. Matrix elasticity directs stem cell lineage specification. Cell. 2006; 126(4):677–689. [PubMed: 16923388]
18. Konttinen YT, Zhao DS, Beklen A, Ma GF, Takagi M, Kivela-Rajamaki M, Ashammakhi N, Santavirta S. The microenvironment around total hip replacement prostheses. Clinical Orthopaedics and Related Research. 2005; (430):28–38. [PubMed: 15662301]
19. Hubbell JA. Biomaterials in Tissue Engineering. Bio-Technology. 1995; 13(6):565–576. [PubMed: 9634795]
20. Ratner BD. A paradigm shift: biomaterials that heal. Polymer International. 2007; 56(10):1183–1185.

21. Benoit DSW, Schwartz MP, Durney AR, Anseth KS. Small functional groups for controlled differentiation of hydrogel-encapsulated human mesenchymal stem cells. Nature Materials. 2008; 7(10):816–823.
22. Brey DM, Erickson I, Burdick JA. Influence of macromer molecular weight and chemistry on poly(beta-amino ester) network properties and initial cell interactions. Journal of Biomedical Materials Research Part A. 2008; 85A(3):731–741. [PubMed: 17896761]
23. Brey DM, Ifkovits JL, Mozia RI, Katz JS, Burdick JA. Controlling poly(beta-amino ester) network properties through macromer branching. Acta Biomaterialia. 2008; 4(2):207–217. [PubMed: 18033746]
24. Ifkovits JL, Burdick JA. Review: Photopolymerizable and degradable biomaterials for tissue engineering applications. Tissue Engineering. 2007; 13(10):2369–2385. [PubMed: 17658993]
25. Tan AR, Ifkovits JL, Baker BM, Brey DM, Mauck RL, Burdick JA. Electrospinning of photocrosslinked and degradable fibrous scaffolds. Journal of Biomedical Materials Research Part A. 2008; 87A(4):1034–1043. [PubMed: 18257065]
26. Ifkovits JL, Padera RF, Burdick JA. Biodegradable and radically polymerized elastomers with enhanced processing capabilities. Biomedical Materials. 2008; 3(3)
27. Hartman EHM, Vehof JWM, de Ruijter JE, Spauwen PHM, Jansen JA. Ectopic bone formation in rats: the importance of vascularity of the acceptor site. Biomaterials. 2004; 25(27):5831–5837. [PubMed: 15172495]
28. Chung C, Beecham M, Mauck RL, Burdick JA. The influence of degradation characteristics of hyaluronic acid hydrogels on in vitro neocartilage formation by mesenchymal stem cells. Biomaterials. 2009; 30(26):4287–4296. [PubMed: 19464053]
29. Burkoth AK, Burdick J, Anseth KS. Surface and bulk modifications to photocrosslinked polyanhydrides to control degradation behavior. Journal of Biomedical Materials Research. 2000; 51(3):352–359. [PubMed: 10880076]
30. Kakudo N, Kusumoto K, Kuro A, Ogawa Y. Effect of recombinant human fibroblast growth factor-2 on intramuscular ectopic osteoinduction by recombinant human bone morphogenetic protein-2 in rats. Wound Repair and Regeneration. 2006; 14(3):336–342. [PubMed: 16808813]
31. Karageorgiou V, Kaplan D. Porosity of 3D biomaterial scaffolds and osteogenesis. Biomaterials. 2005; 26(27):5474–5491. [PubMed: 15860204]
32. Langer R, Vacanti JP. Tissue Engineering. Science. 1993; 260(5110):920–926. [PubMed: 8493529]
33. Hammonds RG, Schwall R, Dudley A, Berkemeier L, Lai C, Lee J, Cunningham N, Reddi AH, Wood WI, Mason AJ. Bone-Inducing Activity of Mature Bmp-2b Produced from a Hybrid Bmp-2a/2b Precursor. Molecular Endocrinology. 1991; 5(1):149–155. [PubMed: 2017189]
34. Sasano Y, Ohtani E, Narita K, Kagayama M, Murata M, Saito T, Shigenobu K, Takita H, Mizuno M, Kuboki Y. Bmps Induce Direct Bone-Formation in Ectopic Sites Independent of the Endochondral Ossification In vivo. Anatomical Record. 1993; 236(2):373–380. [PubMed: 8338240]
35. Burdick JA, Frankel D, Dernell WS, Anseth KS. An initial investigation of photocurable three-dimensional lactic acid based scaffolds in a critical-sized cranial defect. Biomaterials. 2003; 24(9): 1613–1620. [PubMed: 12559821]
36. Brighton CT, Hunt RM. Early histological and ultrastructural changes in medullary fracture callus. Journal of Bone and Joint Surgery. 1991; 73(6):832–847. [PubMed: 2071617]
37. Einhorn, TA.; O'Keefe, RJ.; Buckwalter, JA. Orthopaedic Basic Science: Foundations of Clinical Practice. Rosemont, IL: American Academy of Orthopaedic Surgeons; 2007.

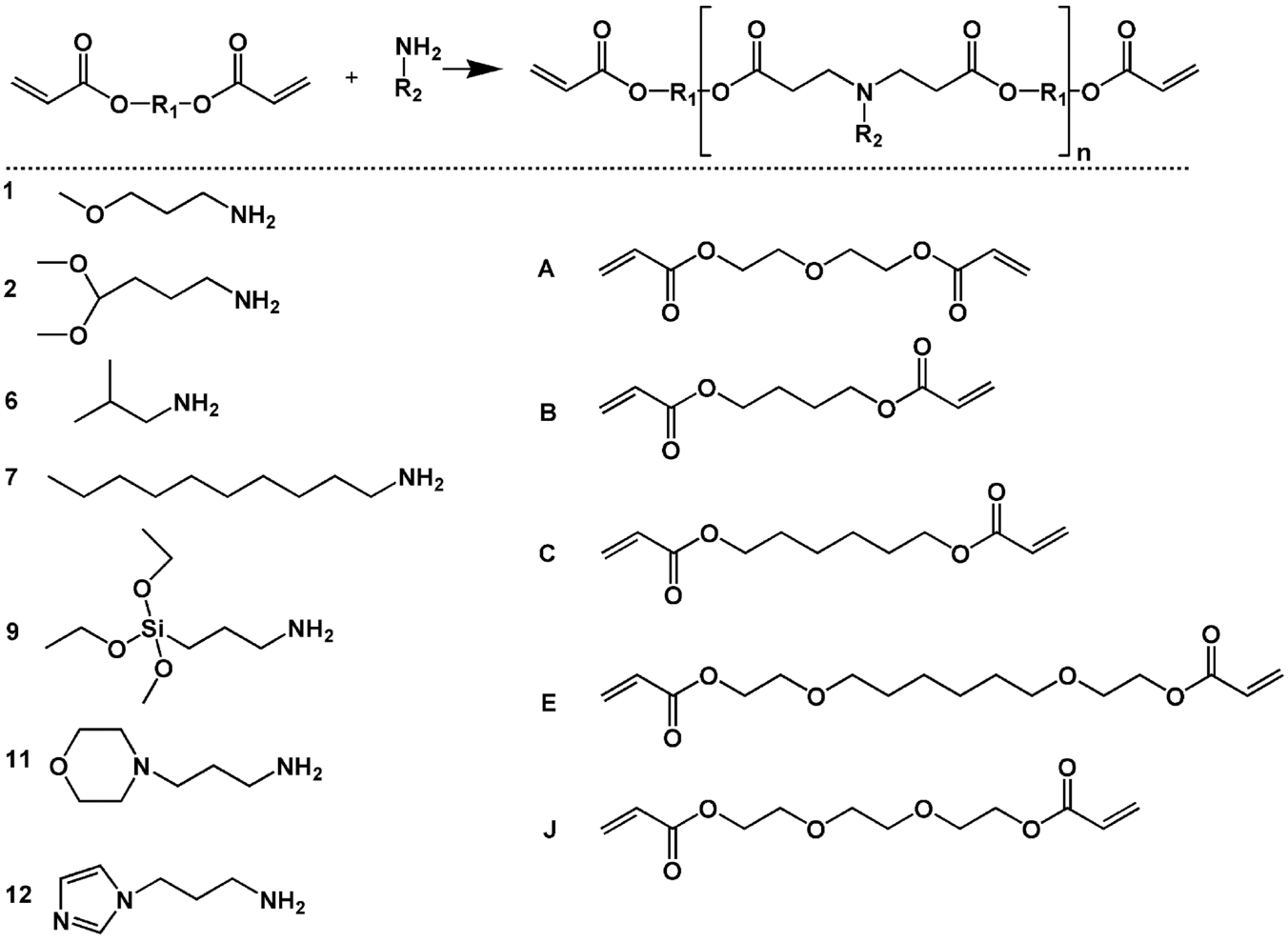


**Figure 1.**

Generalized reaction scheme for the synthesis of photopolymerizable and degradable poly(β-amino ester)s (top) and amines (numbered monomers, determines $R_2$) and diacrylates (lettered monomers, determines $R_1$) used in the synthesis (bottom). The molecule notation is from the original report of the combinatorial library.[8]

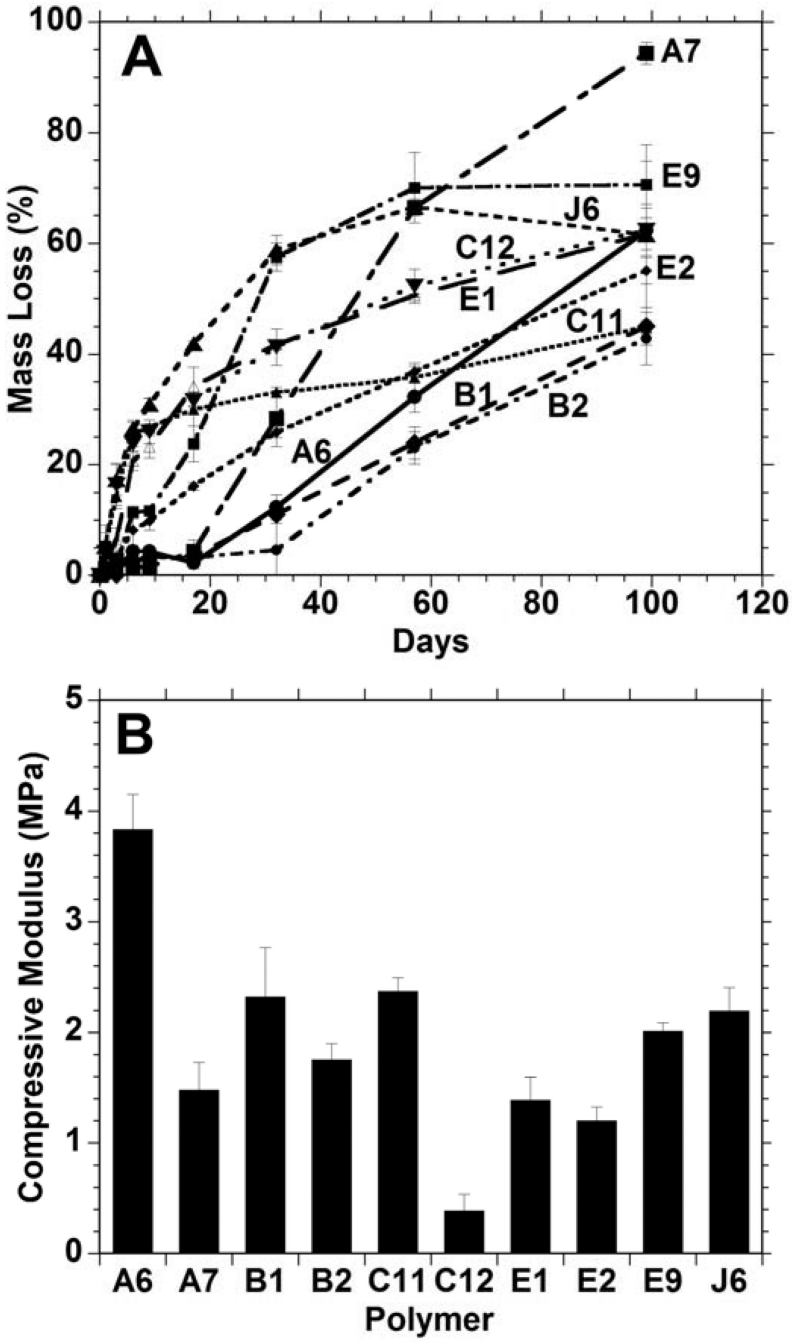


**Figure 2.**

Bulk polymer degradation (A) and compressive moduli (B) of 10 candidate polymers formed from PBAE macromers that met design criteria from the initial combinatorial polymer library. The A6 group possessed a statistically higher ($p<0.05$) modulus than all other groups.

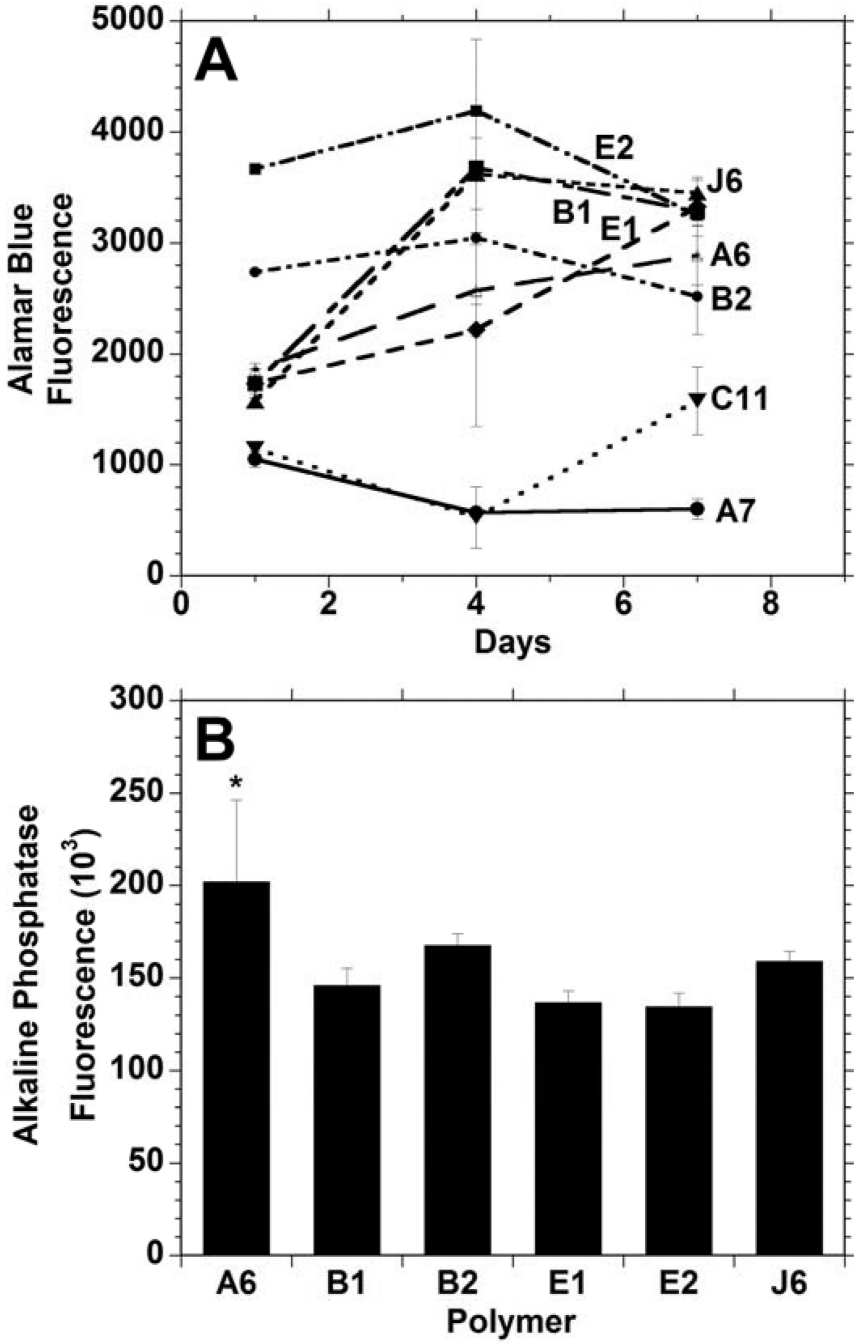


**Figure 3.**

Mesenchymal stem cell viability (measured with Alamar Blue) (A) and alkaline phosphatase activity after 3 days (B) following seeding onto films of candidate polymers formed from PBAE macromers. * indicates significant difference ($p < 0.05$) from all other groups except B2.

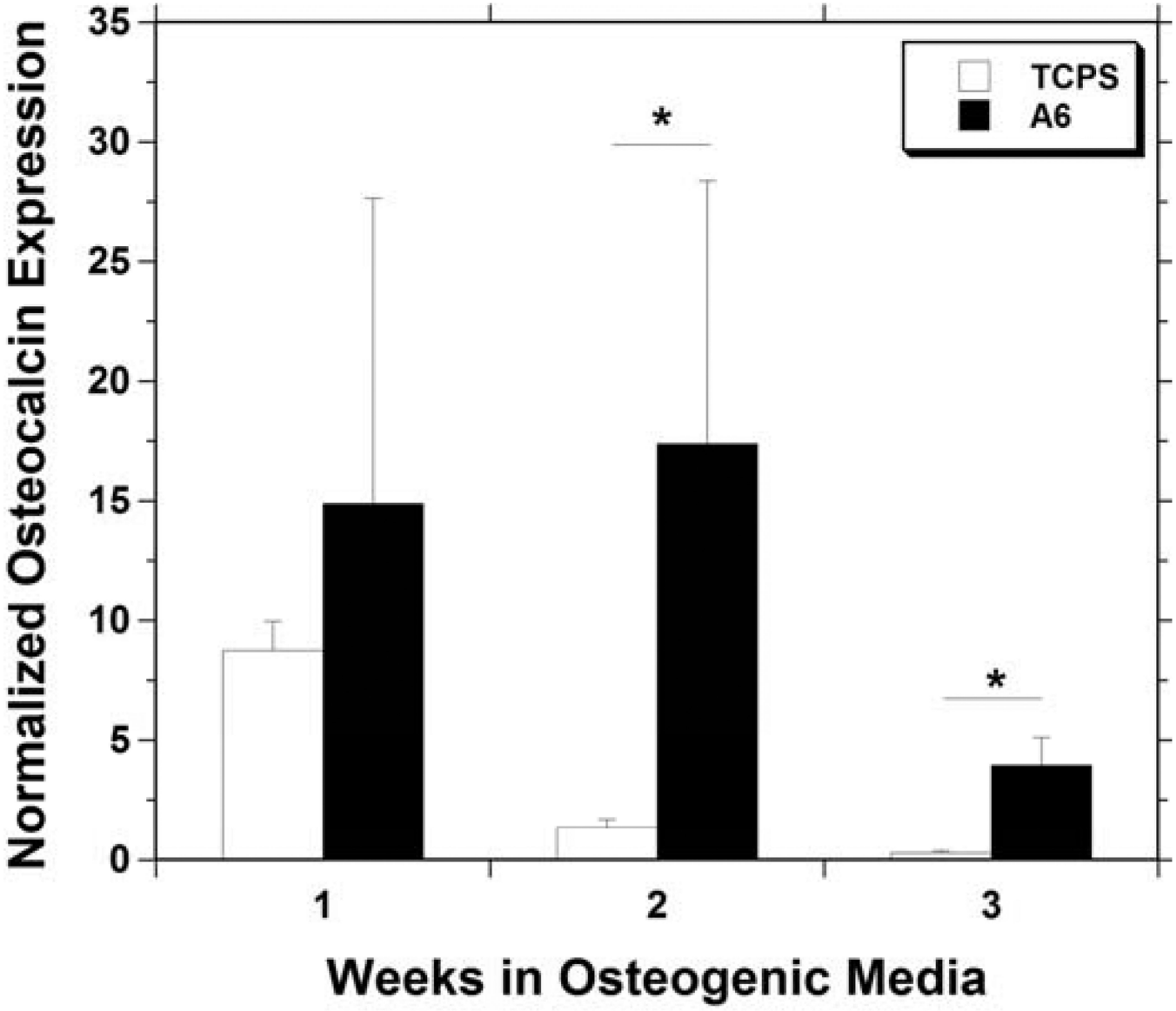


**Figure 4.**

Osteocalcin gene expression in mesenchymal stem cells cultured for up to 3 weeks in osteogenic media on TCPS (white) or A6 thin films (black), normalized to the expression in cells at time of seeding. * indicates a significant difference ($p < 0.05$) between the two groups at that time point.

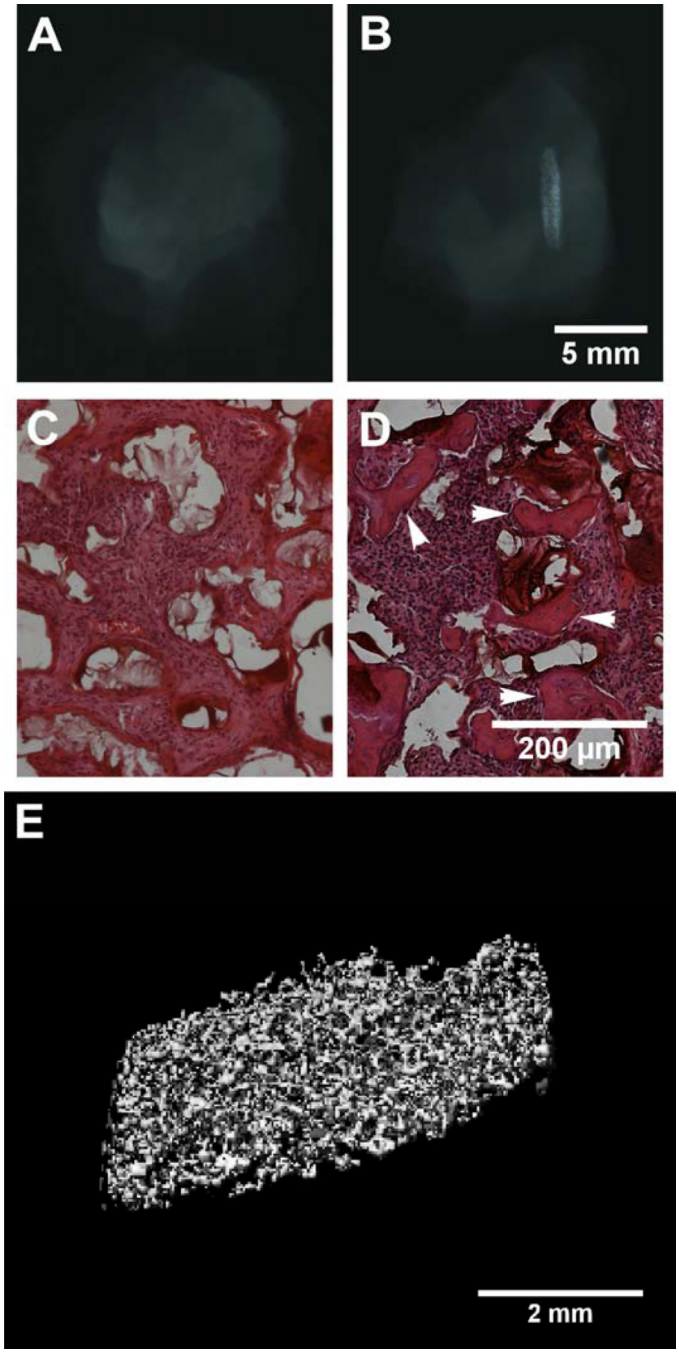


**Figure 5.**
Mass loss profiles of bulk A6 slabs *in vitro* (solid line) or after subcutaneous implantation (dashed line) (A) and representative tissue response to the A6 slabs 4 (B) and 8 weeks (C) after subcutaneous implantation. SEM image of A6 porous scaffolds showing large, interconnected porosity (D) and representative tissue response to A6 porous scaffolds 4 weeks after subcutaneous implantation (E), illustrating complete fibrous tissue infiltration. P = Polymer.

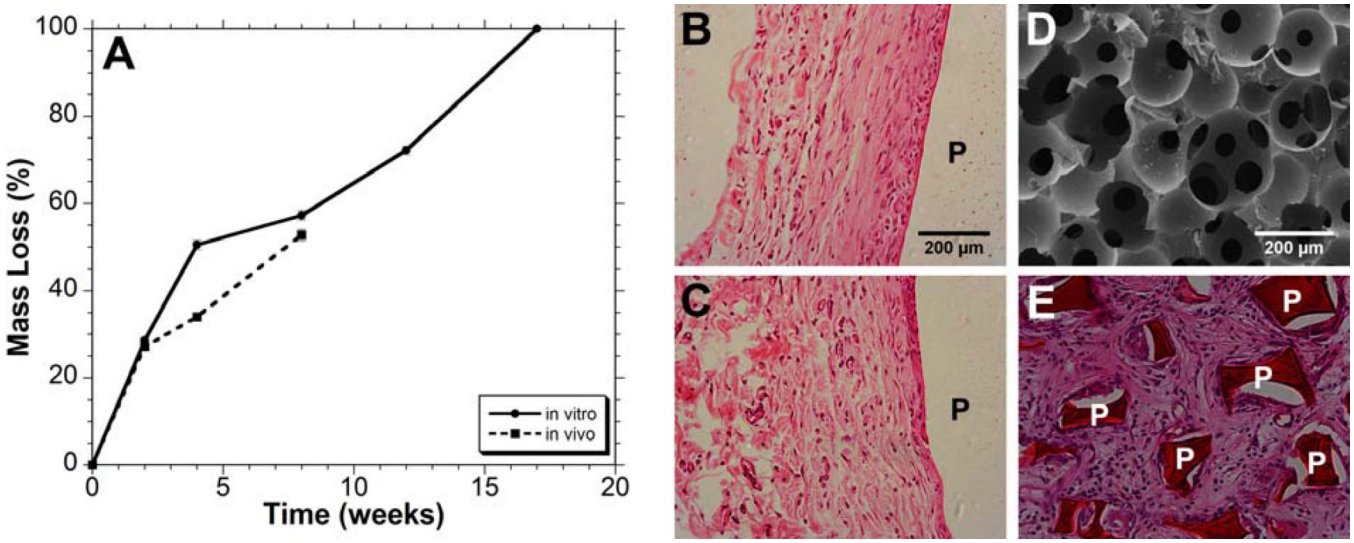


**Figure 6.**

Radiographs (A, B), histology (C, D, mineralized tissue identified with arrows), and micro-CT (E) of A6 scaffolds 3 weeks after intramuscular implantation alone (A, C) or when loaded with BMP-2 (B, D, E). Ectopic mineralized tissue formation was only evident in samples that contained BMP-2 and the tissue formed a porous structure that templated the implanted scaffolds.

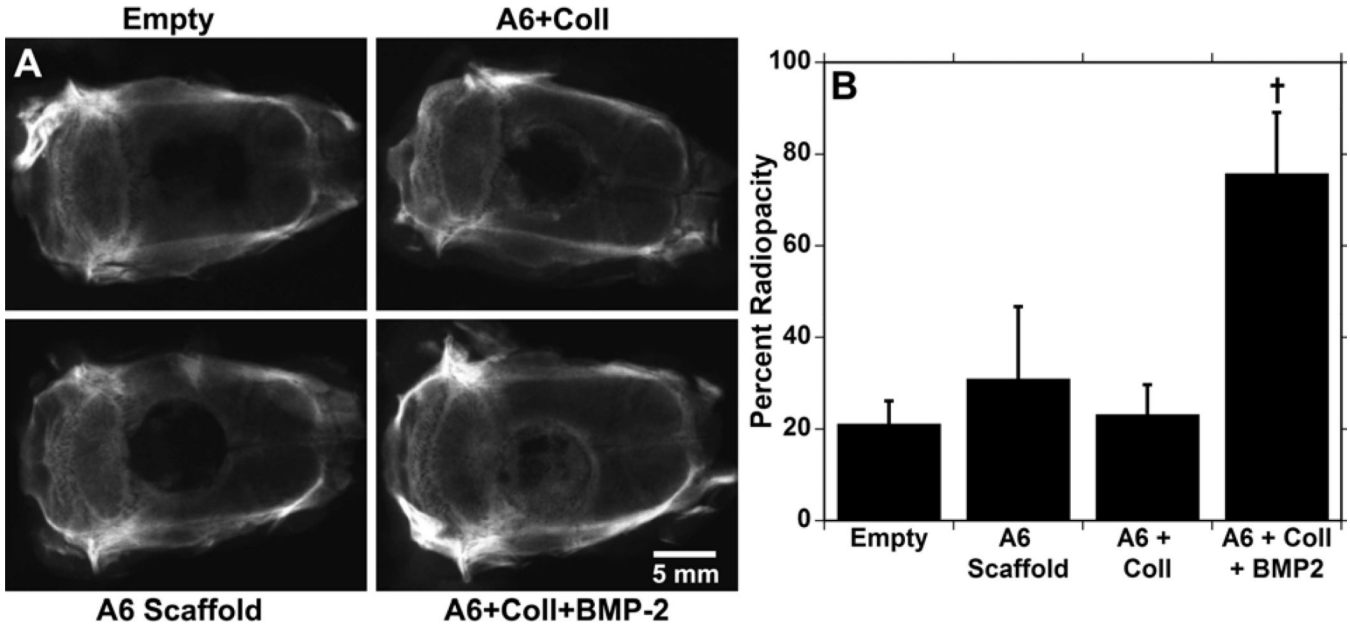


**Figure 7.**

Radiographs of rat calvaria 6 weeks after 8 mm defect creation and either left empty or filled with A6 scaffolds alone or loaded with collagen or collagen and BMP-2 (A). The percent radiopacity of the defect/scaffold compared to intact bone (B). † indicates significant difference ($p < 0.05$) from all other groups.

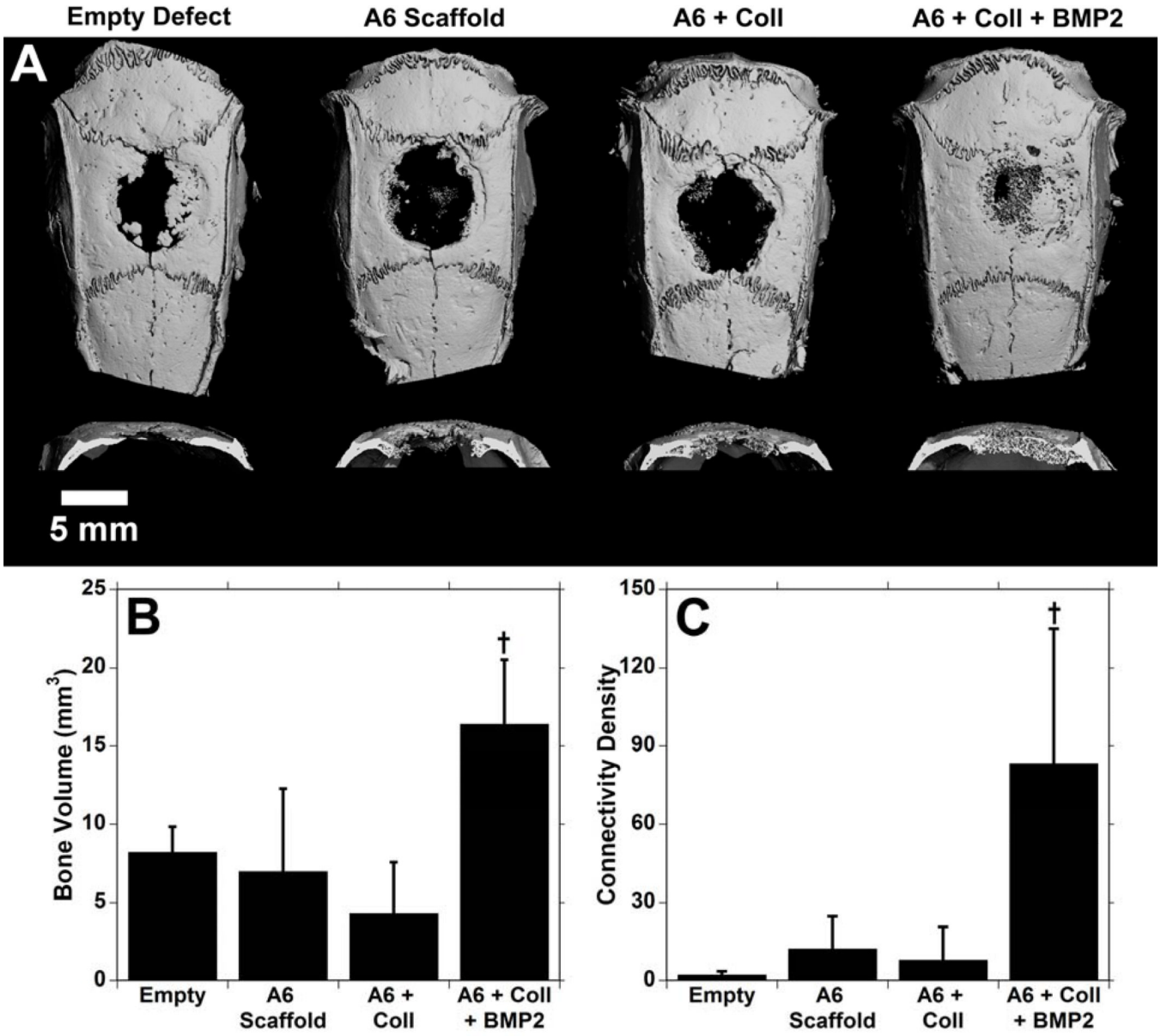


**Figure 8.**

3-dimensional reconstructions (A) and quantification of the bone volume (B) and connectivity index (C) from μCT analysis of the groups 6 weeks after implantation in the calvarial defects. † indicates significant difference ($p < 0.05$) from all other groups.

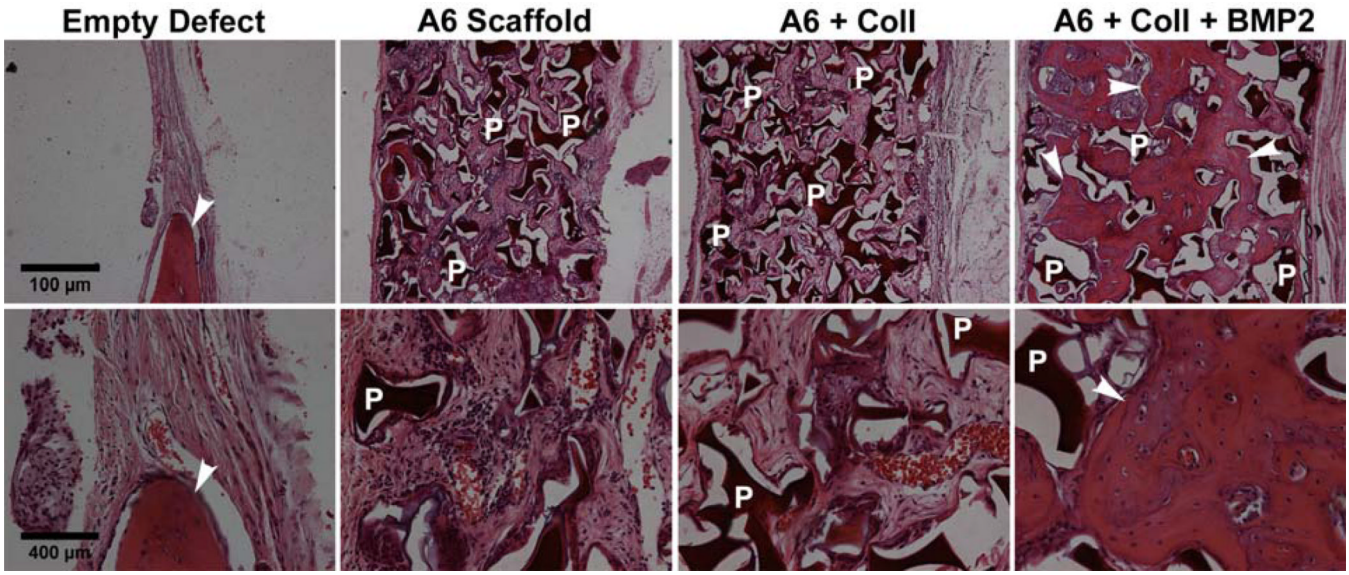


**Figure 9.**
Histological sections of calvarial defects 6 weeks after treatment at two magnifications (top: 5×, bottom: 20×). Only samples with BMP-2 show bone formation throughout the scaffold (labeled with arrows) and polymer scaffold remains at this time point (P = Polymer).

## Table 1

Quantitative PCR primers and probes.

| Gene | Forward Primer | Reverse Primer | Probe |
|---|---|---|---|
| GAPDH | AGGGCTGCTTTTAACTCTGGTAAA | GAATTTGCCATGGGTGGAAT | CCTCAACTACATGGTTTAC |
| Osteocalcin | CTGGCCGCACTTTGCAT | CTGCACCTTTGCTGGACTCT | CACCTGCCTGGCCAGC |